Surface Reaction Probabilities of Silicon Hydride Radicals in SiH 4 /H 2 Thermal Chemical Vapor Deposition

ARTICLE *in* INDUSTRIAL & ENGINEERING CHEMISTRY RESEARCH · MAY 2002

Impact Factor: 2.59 · DOI: 10.1021/ie0107183

3 AUTHORS, INCLUDING:

Dah-Shyang Tsai
National Taiwan University of Science and Te…
144 PUBLICATIONS **1,782** CITATIONS
SEE PROFILE

Yukihiro Shimogaki
The University of Tokyo
278 PUBLICATIONS **1,860** CITATIONS
SEE PROFILE

Surface Reaction Probabilities of Silicon Hydride Radicals in SiH_4/H_2 Thermal Chemical Vapor Deposition

Wei-Chang Hsin and Dah-Shyang Tsai*

Department of Chemical Engineering, National Taiwan University of Science and Technology, 43, Keelung Road, Sec. 4, 106 Taipei, Taiwan

Y. Shimogaki

Department of Materials Engineering, University of Tokyo, 7-3-1 Hongo, Bunkyo-ku, 113-8656 Tokyo, Japan

Surface reaction probabilities of silicon hydride radicals are correlated from measurements of the film thickness profile in trench and the deposition rate in thermal chemical vapor deposition of the SiH_4/H_2 system at 871−913 K. Correlated radical reactive sticking probability RSC_{rd} increases linearly with the fraction of dangling bond ϕ. Experimental data of RSC_{rd} vs ϕ in SiH_4/H_2 and SiH_4/Ar systems fall on the same line when the deposition temperature is the same. The extrapolated RSC_{rd} at $\phi = 1$ of the SiH_4/H_2 system is unity, which indicates that radicals deposit as soon as they impinge on the surface that contains only bare Si atoms. The growing surface reactivity is less than 1 owing to chemisorbed hydrogen. The silicon surface is more passivated in the SiH_4/H_2 system, compared with the SiH_4/Ar system, since molecular hydrogen (sticking coefficient 3.57×10^{-6}) enhances the hydrogen coverage. The radical reaction probability on a hydrogen-saturated Si surface is the RSC_{rd} value extrapolated at $\phi = 0$. The activation energy for radical reaction probability with hydrogen-saturated surface is 4.91 ± 0.06 kcal. CRESLAF simulation results, using this revised surface reaction mechanism and the gas-phase reaction mechanism of Ho, Coltrin, and Breiland, indicate the influences of radicals originate from H_2-$SiSiH_2$, since its concentration is much higher than other radical species.

Introduction

Reaction paths and key elementary steps in the gas-phase and surface reactions of silane chemical vapor deposition (CVD) have been investigated in great detail.[1−6] The first step of silane pyrolysis in thermal CVD is identified as cleaving one hydrogen molecule from SiH_4 to yield a very reactive silylene SiH_2.[7] The insertion of SiH_2 back into SiH_4 yields Si_2H_6, which is further dehydrogenated to generate H_2SiSiH_2 and H_3SiSiH.[1−3] All these silicon-containing species in the gas phase participate in film growth via surface reactions. The sticking coefficients of silane and disilane have been measured, using the surface science techniques.[8−11] The significance of hydrogen desorption kinetics on film growth rate and the surface passivation effects owing to chemisorbed hydrogen have been widely recognized.[12,13]

Unfortunately, the knowledge of interactions between the growing surface and the species of unpaired electron, i.e., silicon hydride radicals, is still insufficient. The radical contribution on film growth is an important factor in film conformality, especially when deposition is under a high temperature or a high silane partial pressure such as rapid thermal CVD. Perrin and Broekhuizen[14] reported the reaction probability of SiH_3 on amorphous Si:H surface varied from 0.1 to 0.2 in the temperature range 40−350 °C. Robertson and Rossi[15] reported the sticking coefficient of SiH_2 on an amorphous hydrogenated silicon surface 0.15, measured by resonance-enhanced multiphoton ionization. Ho, Breiland, and Buss[16] estimated that 94% of SiH in a molecular beam was incorporated in colliding with an amorphous Si:H surface. Sawado et al.[17] estimated the apparent sticking coefficients of SiH and SiH_2 radicals on hydrogenated amorphous Si surface to be 0.84 (373 K) and 0.68 (523 K). Tachibana[18] assumed the sticking coefficient of SiH_3 to be 0.2 and those of SiH_2, SiH, and Si to be 1.0 while simulating the their concentrations in silane RF plasma. Ramalingam et al.[19] reported that 95% reaction probability of SiH with amorphous Si:H surface using quantum chemistry calculation. They also simulated and reported unity reaction probability of SiH_3 with a pristine Si(001) 2×1 surface and a much reduced probability with a H-terminated surface.[20,21] There is little knowledge about the sticking coefficients of Si_2H_4, which are considered important radicals in the gas phase of silane thermal CVD.

Although the knowledge on elementary steps of silane gas-phase and surface reactions is plentiful, piecing together these rate equations to describe the deposition kinetics remains to be a formidable task. In this report, we carry out the poly-Si deposition in the SiH_4/H_2 reaction system and extract the radical reaction probabilities from trench analysis. Compared with the previous study on SiH_4/Ar system, the growing surface is less reactive toward the film-forming species due to the surface hydrogenation of H_2. Effects of surface hydrogenation on radicals sticking coefficient are emphasized and discussed in this work.

Experimental Section

Deposition experiments were carried out in a hot-wall tubular reactor, using the SiH_4/H_2 system with the hot-

* To whom the correspondence should be addressed: e-mail tsai@ch.ntust.edu.tw; Ph 886-2-2737-6618; FAX 886-2-2737-6644.

10.1021/ie0107183 CCC: $22.00
Published on Web 04/04/2002

zone temperature 871, 893, 903, and 913 K and total pressure 3.0, 5.0, and 6.0 Torr. The molar fraction of SiH_4 in the feed stream was fixed at 0.4; therefore, the silane partial pressure was 1.2, 2.0, and 2.4 Torr for total pressure 3.0, 5.0, and 6.0 Torr, respectively. The wall temperature variation in a hot zone of 400 mm was kept within ±1 °C. Clean silicon chips 5 mm wide and 40−45 mm long, cleaved from the Si(100) 6 in. wafer, were placed head-to-tail along the quartz tube in the hot zone. Chips bearing trenches were clued on the rectangular wafer at selected locations. These silicon wafers were thermally oxidized to grow an oxide layer about 10 nm, which served as a marker in film thickness measurement. Film thickness is measured using a field-emission scanning electron microscope, and growth rates are derived from the film thickness data. The film thickness within the trench, especially the one of high aspect ratio, was measured with care. The reactive sticking coefficient of radicals was correlated from simulating the thickness profiles in the trench of high aspect ratio first, and the parameters were confirmed in a trench of lower aspect ratio at the same location. The deposition time was set so that the film thickness was sufficient to carry out critical examinations on fitting parameters. The trench simulation software was based on the Monte Carlo method, which assumed that two film-forming species of widely different reactive sticking coefficients underwent collisions with the solid wall and with each other. The reactive sticking coefficients of radicals were fitted in an Arrhenius-type equation. The software CRESLAF in the CHEMKIN package,[22] using the renewed surface reactions, was applied to calculate the deposition rate variation along the tube and the molar fractions of gas-phase species.

Dangling Bond Fraction of the Growing Silicon Surface

Since a H-terminated surface site is more inert than a surface site of dangling bond and hydrogen is chemisorbed on the silicon surface, reactivity of the growing silicon surface is intimately related to the fraction of its bare silicon atoms. The film-forming species with paired electrons, such as SiH_4, Si_2H_6, and Si_3H_8, have small but finite reaction probabilities with the bare Si atom, and their reaction probabilities with the H-terminated Si atom in the temperature range of poly-Si thermal CVD are negligible.[23] Therefore, the excellent film conformality of silane thermal CVD is a direct consequence of hydrogen passivation and small sticking coefficient of SiH_4.

The surface hydrogenation of carrier gas is of major concern in analyzing the SiH_4/H_2 system. Atomic hydrogen is readily chemisorbed on the clean Si surface and the dissociative adsorption of molecular hydrogen is comparatively difficult, but the hydrogen gas is present in molecular form in this CVD temperature range. Thus, the main hydrogenation contributions in the SiH_4/H_2 system result from the surface reactions between H_2, SiH_4, Si_2H_6, and Si_3H_8 and the bare surface Si atom. The sticking probability for dissociative adsorption of molecular hydrogen is very low at room temperature, less than 10^{-8}. Yet the adsorption exhibits a strong dependence on the substrate temperature; therefore, the H_2 contribution in surface hydrogenation is comparable to those of SiH_4 and Si_2H_6 under the poly-Si deposition temperature. Bratu and Hoffer measured H_2 and D_2 adsorption sticking coefficients on Si(100) 2 × 1[24] and Si(111) 7 × 7,[25] $\eta_{H_2} = 0.1 \exp(-17.3 \text{ kcal}/RT_S)$ and $\eta_{H_2} = 7 \times 10^{-2} \exp(-20.1 \text{ kcal}/RT_S)$, respectively. η_{H_2} is the H_2 sticking probability with a dangling bond, and T_S is the substrate temperature. The sticking probabilities of these two equations are lower than the numbers quoted in a review paper of Greve.[26] The correlated sticking coefficient of H_2 in this work is 3.57×10^{-6}, which is lower than the η_{H_2} of Si(100) 2 × 1 and higher than that of Si(111) 7 × 7 in the temperature range 871−913 K.

The total surface site number of growing silicon S_D is assumed constant, 1.0×10^{15} cm^{-2} (1.661×10^{-9} mol cm^{-2}).[27] This particular site density is higher than that of Si(100) 6.8×10^{14} cm^{-2}, Si(111) 7.8×10^{14} cm^{-2}, Si(110) 9.6×10^{14} cm^{-2}, and less than the average number of Si crystal 1.36×10^{15} cm^{-2}. Each surface site is occupied by either a monohydride SiH(S) or a bare Si atom Si(S). Influences of surface reconstruction of certain crystalline areas and the possibility of SiH_x(S) ($x \geq 2$) are excluded for simplicity. Surface contamination of other atoms is considered negligible. A steady state of surface hydrogen occupation is reached after a very brief time of initial growth. Balancing the hydrogenation and dehydrogenation kinetics yields the fraction of dangling bond ϕ at steady state.

$$SiH_4 + 2Si(S) \rightarrow 2SiH(S) + Si(B) + H_2 \qquad k_1[SiH_4](S_D\phi)^2 \quad (1)$$

$$Si_2H_6 + 2Si(S) \rightarrow 2SiH(S) + 2Si(B) + 2H_2 \qquad k_2[Si_2H_6](S_D\phi)^2 \quad (2)$$

$$Si_3H_8 + 2Si(S) \rightarrow 2SiH(S) + 3Si(B) + 3H_2 \qquad k_3[Si_3H_8](S_D\phi)^2 \quad (3)$$

$$H_2 + 2Si(S) \rightarrow 2SiH(S) \qquad k_4[H_2](S_D\phi)^2 \quad (4)$$

$$SiH(S) \rightarrow Si(S) + {}^1/_2H_2 \qquad k_5S_D(1-\phi) \quad (5)$$

$$\phi = \frac{-k_5 + \sqrt{k_5^2 + 8k_5S_D(k_1[SiH_4] + k_2[Si_2H_6] + k_3[Si_3H_8] + k_4[H_2])}}{4S_D(k_1[SiH_4] + k_2[Si_2H_6] + k_3[Si_3H_8] + k_4[H_2])} \quad (6)$$

The first-order desorption constant $k_5 = 7.9 \times 10^{11} \exp(-45500 \text{ cal}/RT)$, which is taken from the thermal recombinative desorption kinetics of SiH(S) phase on Si(100),[28,29] is also the best fit in simulating the SiH_4/Ar system.[30] The dissociative adsorption of H_2, eq 4, is a factor on surface hydrogenation in the SiH_4/H_2 system but insignificant in the SiH_4/Ar system owing to a much lower hydrogen concentration. If the CRESLAF simulation is repeated in the SiH_4/Ar system with $\eta_{H_2} = 3.57 \times 10^{-6}$, the calculated maximum differences in ϕ are less than 4×10^{-3} with and without eq 4. Arrhenius parameters of the kinetic constants in reactions 1−5 are listed in Table 1.

Although a considerable amount of SiH_4 is converted into Si_2H_6 and other species, and the wall concentrations of SiH_4, Si_2H_6, Si_3H_8, and H_2 vary moderately along the tubular reactor, the fraction of dangling bond changes just a little. The calculated ϕ values of three horizontal positions, where trenches are located, are plotted against the corresponding deposition temperature and pressure in Figure 1A. Under a pair of temperature and pressure,

Table 1. Elementary Steps Involved in Surface Reactions of SiH_4/H_2 Thermal CVD[a]

elementary surface reaction	A	β	E_A
$SiH_4 + 2Si(S) \rightarrow 2SiH(S) + Si(B) + H_2$	8.39×10^{26}	0.0	37450
$Si_2H_6 + 2Si(S) \rightarrow 2SiH(S) + 2Si(B) + 2H_2$	8.39×10^{27}	0.0	37450
$Si_3H_8 + 2Si(S) \rightarrow 2SiH(S) + 3Si(B) + 3H_2$	8.39×10^{27}	0.0	37450
$H_2 + 2Si(S) \rightarrow 2SiH(S)$	3.32×10^{15}	0.5	0
$SiH(S) \rightarrow Si(S) + {}^1/_2H_2$	7.9×10^{11}	0.0	45500
sticking coeffs of radicals			
$SiH_2 + Si(S) \Rightarrow Si(B) + Si(S) + H_2$	1.0	0.0	0.0
$Si + Si(S) \Rightarrow Si(B) + Si(S)$	1.0	0.0	0.0
$H_2SiSiH_2 + Si(S) \Rightarrow 2Si(B) + Si(S) + 2H_2$	1.0	0.0	0.0
$H_3SiSiH + Si(S) \Rightarrow 2Si(B) + Si(S) + 2H_2$	1.0	0.0	0.0
$SiH_2 + SiH(S) \Rightarrow Si(B) + SiH(S) + H_2$	11.8	0.0	4910.0
$Si + SiH(S) \Rightarrow Si(B) + SiH(S)$	11.8	0.0	4910.0
$H_2SiSiH_2 + SiH(S) \Rightarrow 2Si(B) + SiH(S) + 2H_2$	11.8	0.0	4910.0
$H_3SiSiH + SiH(S) \Rightarrow 2Si(B) + SiH(S) + 2H_2$	11.8	0.0	4910.0

[a] The rate constants are expressed as $AT^{\beta} \exp(-E_A/RT)$; parameters are given in terms of moles, cm, cal, K. Also listed are the reaction probabilities of radicals with SiH(S) and Si(S). Elementary gas-phase reactions of Ho, Coltrin, and Breiland (ref 1) are used in combination with the above surface reaction scheme in CRESLAF simulation.

small differences in ϕ among three positions are within experimental error. The constant ϕ value of three different positions is the consequence of SiH_4 loss compensated by Si_2H_6 and Si_3H_8, plus an almost constant H_2 concentration in the gas phase. The reactivity of growing surface, symbolized by ϕ, increases with the deposition temperature and decreases with the total pressure.

Besides surface hydrogenation, eq 1 provides the probability information concerning silane deposition. Sticking coefficient of silane η_{SiH_4} is defined as the SiH_4 reaction probability with a bare surface silicon atom. The reactive sticking coefficient of silane RSC_{SiH_4} is the SiH_4 reaction probability in each impingement with the Si surface. Not every impingement on surface will meet two Si(S); hence, the reactive sticking coefficients of SiH_4, Si_2H_6, and Si_3H_8 are their sticking coefficients multiplied with ϕ^2, according to eqs 1−3. The relation between the reaction constant k_1 and the sticking coefficient η_{SiH_4} is

$$k_1 = \frac{\eta_{SiH_4}}{{S_D}^2}\sqrt{\frac{RT}{2\pi M_{SiH_4}}} \qquad (7a)$$

Similarly, the H_2 sticking coefficient η_{H_2} is related to k_5.

$$k_5 = \frac{\eta_{H_2}}{{S_D}^2}\sqrt{\frac{RT}{2\pi M_{H_2}}} \qquad (7b)$$

The film-forming species SiH_4, Si_2H_6, and Si_3H_8 have low sticking probabilities, which are widely different from those of the radicals SiH_2, H_2SiSiH_2, H_3SiSiH, and Si; we postulate two species in simulating the thickness contours of trenches. One species is of low reactive sticking coefficient RSC_{low} and the other of high reactive sticking coefficient RSC_{rd}. The value of RSC_{low} is calculated at each trench location, under the assumption that the molar fractions of SiH_4, Si_2H_6, and Si_3H_8 above

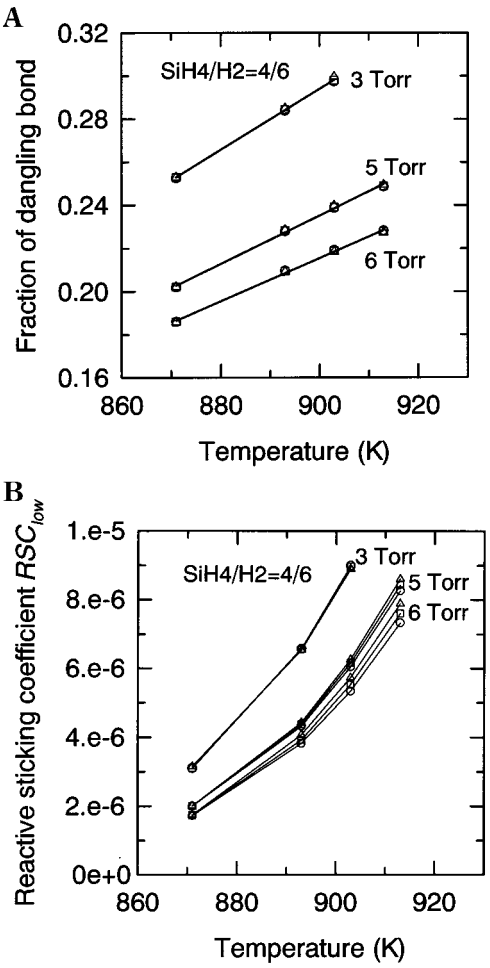

Figure 1. (A) Fraction of dangling bond of growing surface ϕ vs deposition temperature. There are three calculated ϕ values (○, □, △), using eq 6 and simulated CRESLAF concentrations of SiH_4, Si_2H_6, Si_3H_6, and H_2, for each pair of deposition temperature and pressure. These three ϕ's are located at the trench positions. (B) RSC_{low} of low sticking coefficient species vs deposition temperature. Calculations of RSC_{low} are based on eq 8, simulated CRESLAF concentrations of SiH_4, Si_2H_6, Si_3H_6, and ϕ values in (A). Differences among three RSC_{low} (○, □, △) at three trench positions increase with temperature and total pressure.

the trench are the wall concentrations of these species since the maximum distance between Si surface and tube wall is only 0.28 mm. RSC_{low} is defined in the following equation.

$$RSC_{low} = (\eta_{SiH_4}\phi^2[SiH_4] + 2\eta_{Si_2H_6}\phi^2[Si_2H_6] + 3\eta_{Si_3H_8}\phi^2[Si_3H_8])/[SiH_4]_0 \qquad (8)$$

in which $[SiH_4]_0$ is the silane inlet concentration. The values of RSC_{low} at different trench locations are plotted in Figure 1B. Note that variations of RSC_{low} with temperature and pressure are similar those of ϕ, but the differences due to horizontal positions are somewhat larger in RSC_{low}. The RSC_{low} value is on the order of 10^{-6} and increases with the horizontal position.

Estimation of the most appropriate η_{H_2} involves a trial-and-error procedure. The first step is to select a sticking coefficient for dissociative adsorption of H_2; a number between those η_{H_2} values of Si(100)2 × 1 and Si(111)7 × 7 is a reasonable guess. The second step is to calculate the fraction of dangling bond for each deposition condition, which involves running the

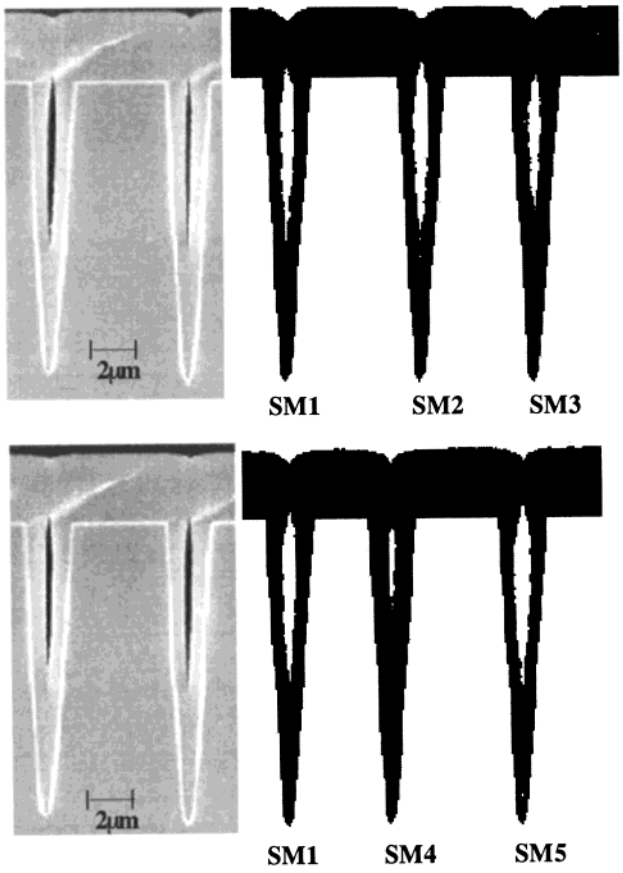

Figure 2. Comparison of trench thickness contours in the micrograph and simulation results with various radical parameters. Silane CVD at 903 K and 5 Torr, the trenches located at 20.8 cm, $RSC_{low} = 6.27 \times 10^{-6}$. (A, top) Fixed RSC_{rd} 0.82, and three different H_2SiSiH_2 partial pressure 2.11×10^{-5} (SM1), 2.21×10^{-5} (SM2), and 2.01×10^{-5} Torr (SM3). (B, bottom) Fixed H_2SiSiH_2 partial pressure 2.11×10^{-5} Torr and three different RSC_{rd} 0.82 (SM1), 0.78 (SM4), and 0.86 (SM5). The simulated thickness contour SM1 is identified as the best resemblance.

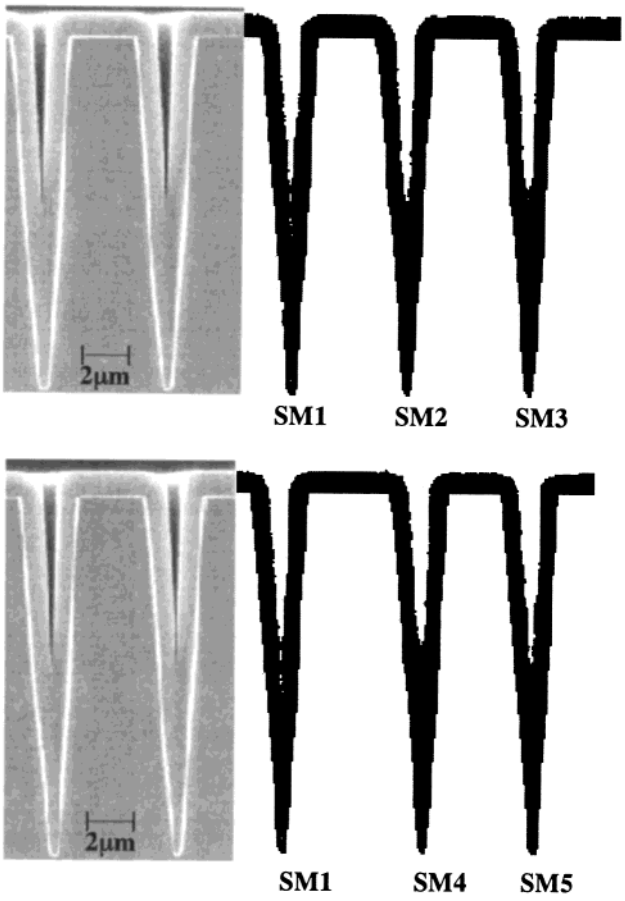

Figure 3. Comparison of trench thickness contours in the micrograph and simulated contours using different radical parameters. Silane CVD at 903 K and 3 Torr, the trenches located at 17 cm, $RSC_{low} = 8.988 \times 10^{-6}$. (A, top) Fixed RSC_{rd} 0.836 and three H_2SiSiH_2 partial pressure 2.436×10^{-6} (SM1), 2.556×10^{-6} (SM2), and 2.316×10^{-6} Torr (SM3). (B, bottom) Fixed H_2SiSiH_2 partial pressure 2.436×10^{-6} Torr, and three RSC_{rd} 0.836 (SM1), 0.796 (SM4), and 0.876 (SM5). The simulated thickness profile SM1 exhibits the finest resemblance.

CRESLAF software, with a full description of wall temperature and a fixed total pressure, to retrieve the local molar fraction of SiH_4, Si_2H_6, Si_3H_8, and H_2. Although Figure 1A indicates that ϕ hardly changes along the reactor, but the selection of η_{H_2} can influence the calculated ϕ value. The value of RSC_{low} is even more sensitive to the choice of η_{H_2}. The third step is to extract the molar fraction and the RSC_{rd} value of radicals from trench simulations and also calculate the local deposition rate. The trench simulation determines the relative weights in deposition between low-sticking-coefficient species and radicals. The sum of deposition contributions from low-sticking-coefficient species and radicals will be equivalent to the local deposition rate. An iteration procedure through steps 1−3 resolves the appropriate η_{H_2}. As a final check, the effects of neglecting η_{H_2} in the SiH_4/Ar system are calculated; the influence is very small due to the low hydrogen concentration.

Sticking Coefficients and Concentrations of Radicals at Trench Sites

Existence of radicals in the gas phase enhances the film deposition rate but impairs the film conformality in thermal CVD. Influences of radicals are more visible in a deep trench than a trench of low aspect ratio. Two geometrically different examples are shown in Figures 2 and 3. The trenches in Figure 2, with an aspect ratio more than 10, are placed at 20.8 cm away from the reactor entrance and deposited at 903 K and 5 Torr. Figure 2A compares the simulated thickness profiles of three radical (H_2SiSiH_2) partial pressure 2.11×10^{-5}, 2.21×10^{-5}, and 2.01×10^{-5} Torr under a fixed RSC_{rd} of 0.82. The film contour of partial pressure 2.11×10^{-5} Torr fits the experimental result. When 2.21×10^{-5} Torr is assumed, the trench is sealed prematurely at the opening; therefore, the keyhole is longer and wider. When a lower radical concentration is assumed at 2.01×10^{-5} Torr, more Si is deposited in trench before being sealed and the keyhole is smaller. On the other hand, with the H_2SiSiH_2 partial pressure fixed at 2.11×10^{-5} Torr, three simulated profiles of $RSC_{rd} = 0.82$, 0.78, and 0.86 are illustrated in Figure 2B. The smaller $RSC_{rd} = 0.78$ generates a smaller keyhole, while the larger $RSC_{rd} = 0.86$ creates a larger keyhole. Figure 3 illustrates another type of thickness profile in the deep trench, which is placed at 17 cm and deposited at 903 K and total pressure 3 Torr. Two films on the side wall merge at the bottom tip; therefore, the opening width or the bottom position is sensitive to the simulation parameters. Figure 3A,B indicates that a higher radical partial pressure or a higher RSC_{rd} value forms a trench

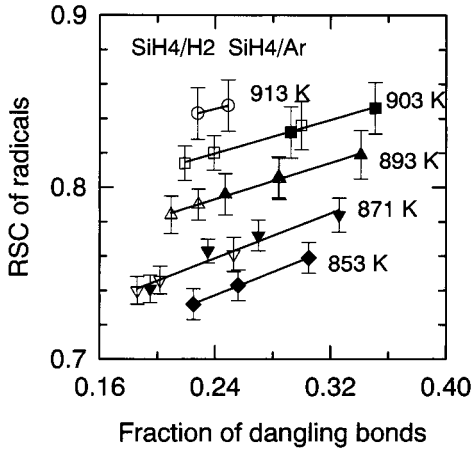

Figure 4. Reactive sticking coefficient of radicals RSC_{rd} vs fraction of dangling bond ϕ in silane thermal CVD. Hollow symbols (○, □, △, ▽) are data of SiH_4/H_2 CVD, and solid symbols (■, ▲, ▼, ◆) are data of SiH_4/Ar CVD.

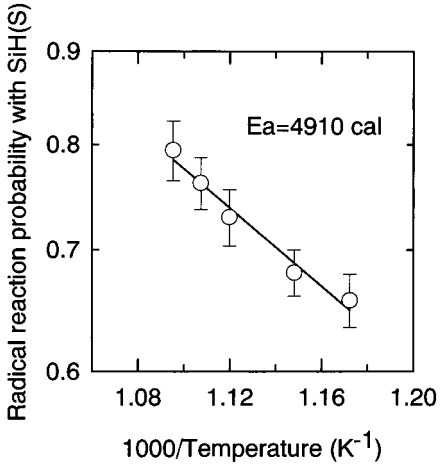

Figure 5. Arrhenius plot of radical reaction probability with hydrogen-terminated silicon η_{rd}. The data points are the intercepts of eq 9 at $\phi = 0$.

of wider opening. A lower radical concentration or a smaller RSC_{rd} value creates a more filled-up trench.

Figure 4 is the plot of reactive sticking coefficient of radicals RSC_{rd} vs the fraction of dangling bond ϕ. The hollow symbols represent experimental data taken from the SiH_4/H_2 reaction system, while the solid symbols were data of the SiH_4/Ar system. Owing to the high molar fraction of hydrogen in the gas phase, ϕ in SiH_4/H_2 is generally less than that in SiH_4/Ar at the same temperature, but both systems exhibit a linear dependence of RSC_{rd} on ϕ. The following equations correlate the experimental data of two systems.

$$RSC_{rd} = 0.794 + 0.213\phi \qquad 913\ K \qquad (9a)$$

$$RSC_{rd} = 0.762 + 0.243\phi \qquad 903\ K \qquad (9b)$$

$$RSC_{rd} = 0.730 + 0.265\phi \qquad 893\ K \qquad (9c)$$

$$RSC_{rd} = 0.680 + 0.328\phi \qquad 871\ K \qquad (9d)$$

$$RSC_{rd} = 0.657 + 0.337\phi \qquad 853\ K \qquad (9e)$$

The above correlation equations indicate that RSC_{rd} bears a linear dependence on ϕ, and the extrapolated RSC_{rd} value is unity when ϕ equals 1 at temperatures 913−853 K. Physically, this limiting RSC_{rd} at $\phi = 1$ means that radicals deposit in every impingement if the surface has bare surface Si atoms only. The hydrogen coverage reduces the radical reactive sticking coefficient owing to lower reactivity with the hydrogen-terminated silicon site. The other limiting RSC_{rd} at $\phi = 0$ represents the reaction probability with the Si surface saturated with chemisorbed hydrogen. The RSC_{rd} at $\phi = 0$ could be interpreted as the reaction probability with SiH(S). The temperature dependence of RSC_{rd} at $\phi = 0$ is illustrated in Figure 5. The Arrhenius equation for reaction probability with SiH(S) η_{rd} is

$$\eta_{rd} = 11.8 \exp(-4910 \pm 60\ \text{cal}/RT) \qquad (10)$$

The above equation of reaction probability with SiH(S) η_{rd} is valid between surface temperature 853 and 913 K. The physical upper limit of η_{rd} is unity.

In the literature, the reactive sticking coefficients of radicals are estimated between 1.0 and 0.1.[14−20] Our correlated RSC_{rd} values are near the sticking coefficients of SiH and SiH_2, reported by Sawado et al.,[17] lower than that of SiH reported by Ho, Breiland, and Buss.[16] Our result of extrapolated unity RSC_{rd} at pristine Si surface is consistent with the simulation result of Ramalingam et al. on SiH and SiH_3 interaction with bare Si atom. Our extrapolated reaction probability SiH(S) η_{rd} seems to be higher than their simulation results.[19,20]

Parts A, B, C, and D of Figure 6 illustrate the partial pressures of H_2SiSiH_2 at the trench locations at 913, 903, 893, and 871 K, respectively. The partial pressure of radicals generally increases with the temperature and the total pressure. The trenches are placed in the region where the deposition rate increases; therefore, the correlated H_2SiSiH_2 partial pressure also increases with the axial position. Since the deposition is operated under a high silane partial pressure, the film growth in the region of declining deposition rate is troubled with fine particles. Therefore, most of film growth rate data are measured in the increasing region only a few growth rates in the declining region are measured. Figure 7 compares the measured deposition rates at 893 K and 5 Torr, and two simulated deposition rates, using CRESLAF with the surface reaction mechanism listed in Table 1. The difference between the calculated deposition rates of $RSC_{rd} = 1$ and RSC_{rd} of eqs 9 is small; it arises near the location of maximum deposition rate. The simulation results, using eqs 9, fit the experimental data slightly better.

Figure 8 is the CRESLAF-simulated molar fractions of film-forming species in the gas phase of SiH_4/H_2 CVD at 893 K and 5 Torr. Concentrations of these species, except SiH_4, increase first and then decrease, and their maximum locations coincide with the maximum point of deposition rate. The molar fractions of film-forming species rank in the following order: $SiH_4 > Si_2H_6 > Si_3H_8 > H_2SiSiH_2 > SiH_2 > H_3SiSiH > Si$. Being the least reactive radical, H_2SiSiH_2 is the most abundant radical, and its concentration is higher than the next most abundant radical SiH_2 by 2 orders of magnitude. Although the correlated RSC_{rd} is a parameter that stands for H_2SiSiH_2, SiH_2, H_3SiSiH, and Si all together, considering the dominating abundance of H_2SiSiH_2 and the near unity RSC_{rd} value, the radicals in the present temperature and pressure range are well represented by H_2SiSiH_2.

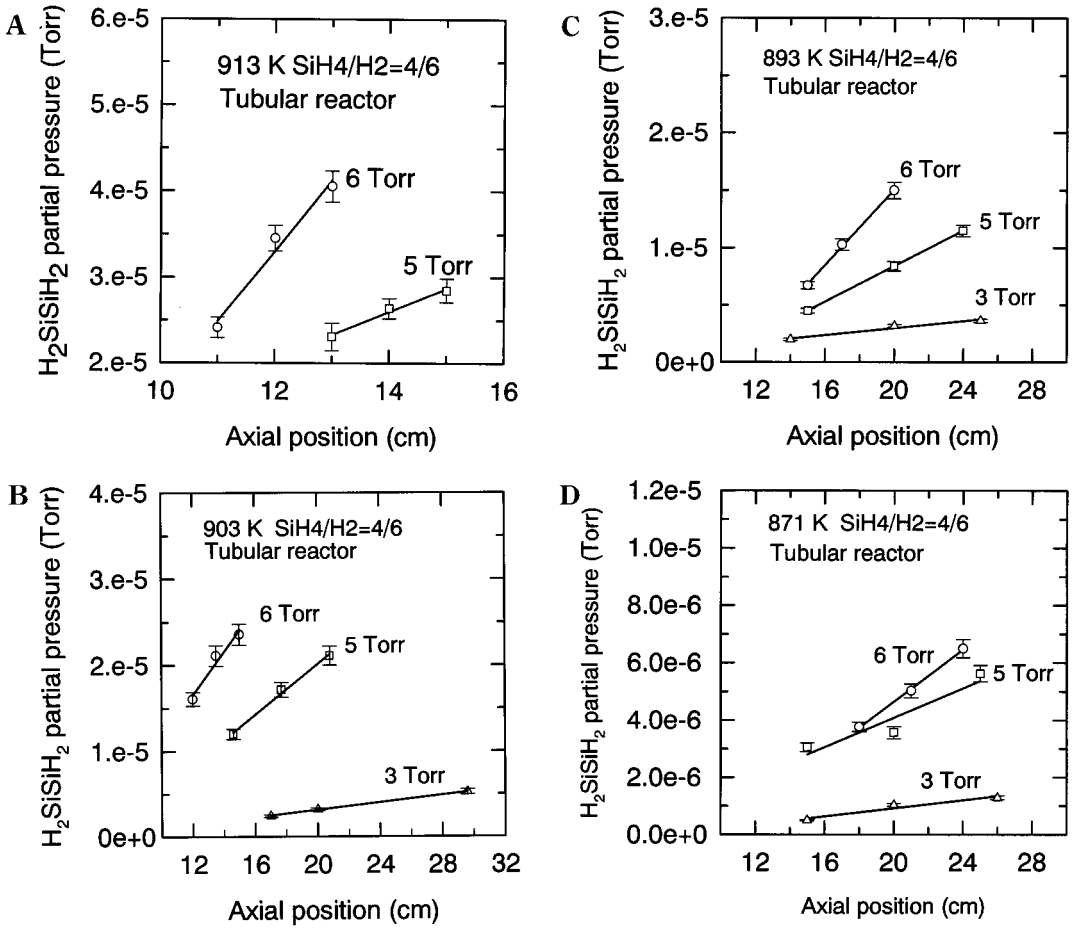

Figure 6. Correlated H_2SiSiH_2 partial pressures at different trench locations, in SiH_4/H_2 CVD under various deposition temperature: (A) 913 K, (B) 903 K, (C) 893 K, and (D) 871 K.

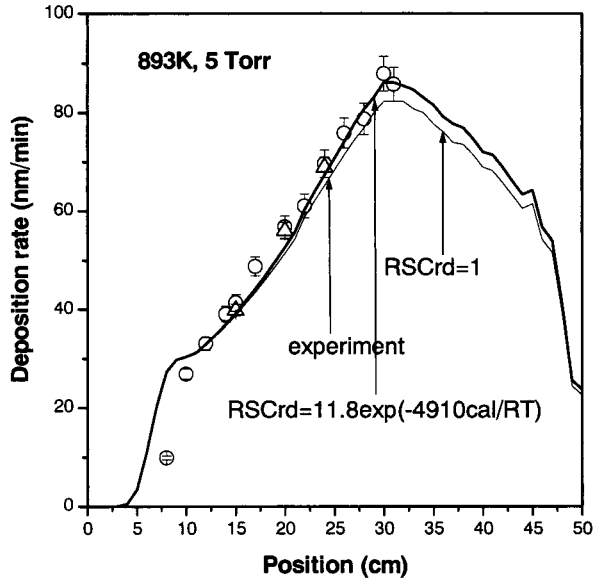

Figure 7. Deposition rate vs axial position in SiH_4/H_2 CVD at 893 K and 5 Torr. Two CRESLAF simulations using $RSC_{rd} = 1.0$ (—) and RSC_{rd} = eq 9 (—) are compared with experimental data. The data points (○) are measured on plane surface; the data points (△) are measured on trench shoulder. Deposition rates at locations beyond the maximum point are not reported, since ultrafine particles appear around 35 cm.

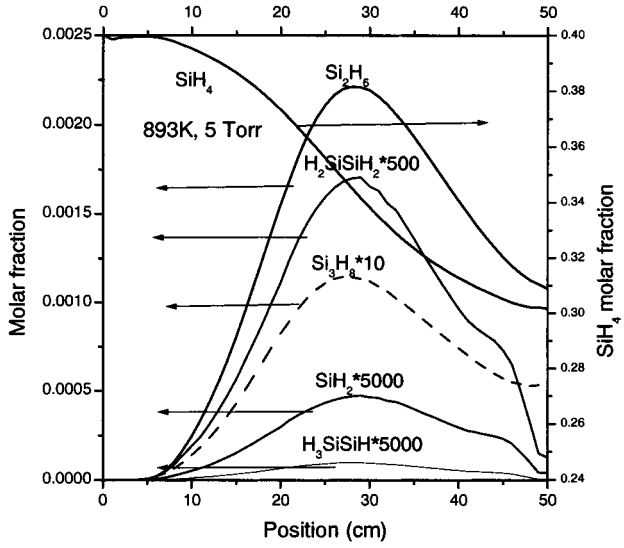

Figure 8. Typical CRESLAF-simulated molar fractions of SiH_4, Si_2H_6, Si_3H_8, H_2SiSiH_2, SiH_2, and H_3SiSiH vs the axial position in SiH_4/H_2 CVD. The simulation implements the gas-phase reaction mechanism suggested by Ho, Coltrin, and Breiland (ref 1) and the surface reaction mechanism listed in Table 1.

Summary

Surface hydrogenation by molecular hydrogen plays an important role in the thermal CVD of SiH_4/H_2 system. A trial-and-error procedure, iteration through 33 deep-trench simulations deposited at 913, 903, 893, and 871 K and total pressure 6, 5, and 3 Torr, is applied to find the most appropriate dissociative sticking coefficient. As the previous study on deposition of the SiH_4/Ar system, the correlated radical reactive sticking

coefficient RSC_{rd} can be separated into two reaction probabilities; one is the probability of depositing on the bare surface Si atom, and the other is the probability of depositing on the hydrogen-terminated Si atom. The former reaction has a unity probability, and the latter probability is less than 1, which is correlated by 11.8 $\exp(-4910 \pm 60\ \text{cal}/RT)$.

The correlated radical sticking coefficients are included in the surface reaction mechanism and applied in the CRESLAF simulation to check the consistency with other experimental data. The CRESLAF simulation result suggests that the radical is H_2SiSiH_2.

Acknowledgment

The authors are grateful to National Science Council of Taiwan for the financial support through Project NSC90-2214-E011-017.

Literature Cited

(1) Ho, P.; Coltrin, M. E.; Breiland, W. G. Laser-Induced Fluorescence Measurements and Kinetic Analysis of Si Atom Formation in a Rotating Disk Chemical Vapor Deposition Reactor. *J. Phys. Chem.* **1994**, *98*, 10138.

(2) Onischuk, A. A.; Strunin, V. P.; Ushakova, M. A.; Panfilov, V. N. Studying of Silane Thermal Decomposition Mechanism. *Int. J. Chem. Kinet.* **1998**, *30*, 99.

(3) Weerts, W. L. M.; de Croon, M. H. J. M.; Marin, G. B. The Kinetics of the Low-Pressure Chemical Vapor Deposition of Polycrystalline Silicon from Silane. *J. Electrochem. Soc.* **1998**, *145*, 1318.

(4) Coltrin, M. E.; Kee, R. J.; Miller, J. A. A Mathematical Model of Silicon Chemical Vapor Deposition. *J. Electrochem. Soc.* **1986**, *133*, 1206.

(5) Weerts, W. L. M.; de Croon, M. H. J. M.; Marin, G. B. Low-Pressure Chemical Vapor Deposition of Polycrystalline Silicon. *J. Electrochem. Soc.* **1997**, *144*, 3213.

(6) Rauscher, H. The Interaction of Silanes with Silicon Single-Crystal Surfaces: Microscopic Processes and Structures. *Surf. Sci. Rep.* **2001**, *42*, 207.

(7) Moffatt, H. M.; Jensen, K. F.; Carr, R. W. Estimation of the Arrhenius Parameters for $SiH_4 = SiH_2 + H_2$ by a Nonlinear Regression Analysis of the Forward and Reverse Reaction Rate Data. *J. Phys. Chem.* **1991**, *95*, 145.

(8) Hu, X. F.; Xu, Z.; Lim, D.; Downer, M. C.; Parkinson, P. S.; Gong, B.; Hess, G.; Ekerdt, J. G. In-Situ Optical Second-Harmonic-Generation Monitoring of Disilane Adsorption and Hydrogen Desorption During Epitaxial Growth on Si(001). *Appl. Phys. Lett.* **1997**, *71*, 1376.

(9) Braun, J.; Rauscher, H.; Behm, R. J. Adsorption of Disilane on Si(111) 7 × 7 and Initial Stage of CVD Growth. *Surf. Sci.* **1998**, *416*, 226.

(10) Tsukidate, Y.; Suemitsu, M. Adsorption of SiH_4 or Si_2H_6 on P/Si(100) at Room Temperatures. *Appl. Surf. Sci.* **1998**, *130*−*132*, 282.

(11) Buss, R. J.; Ho, P.; Breiland, W. G.; Coltrin, M. E. Reactive Sticking Coefficients for Silane and Disilane on Polycrystalline Silicon. *J. Appl. Phys.* **1988**, *63*, 2808.

(12) Oura, K.; Lifshits, V. G.; Saranin, A. A.; Zotov, A. V.; Katayama, M. Hydrogen Interaction with Clear and Modified Silicon Surfaces. *Surf. Rep.* **1999**, *35*, 1.

(13) Jasinski, J. M.; Gates, S. M. Silicon Chemical Vapor Deposition One Step at a Time. *Acc. Chem. Res.* **1991**, *24*, 9.

(14) Perrin, J.; Boekhuizen, T. Surface Reaction and Recombination of the SiH_3 Radical on Hydrogenated Amorphous Silicon. *Appl. Phys. Lett.* **1987**, *50*, 433.

(15) Robertson, R. M.; Rossi, M. J. Atom and Radical Surface Sticking Coefficients Measured Using Resonance-Enhanced Multiphoton Ionization. *J. Chem. Phys.* **1989**, *91*, 5037.

(16) Ho, P.; Breiland, W. G.; Buss, R. J. Laser Studies of the Reactivity of SiH with the Surface of a Depositing Film. *J. Chem. Phys.* **1989**, *91*, 2627.

(17) Sawado, Y.; Akiyama, T.; Ueno, T.; Kamisako, K.; Kuroiwa, K.; Tarui, Y. Contributions of Silicon-Hydride Radicals to Hydrogenated Amorphous Silicon Film Formation in Windowless Photochemical Vapor Deposition. *Jpn. J. Appl. Phys.* **1994**, *33* (Part 1), 950.

(18) Tachibana, K. In Situ Investigations of Radical Kinetics in the Deposition of Hydrogenated Amorphous Silicon Films. *Mater. Sci. Eng.* **1993**, *B17*, 68.

(19) Ramalingam, S.; Maroudas, D.; Aydil, E. S. Interactions of SiH radicals with Silicon Surfaces: An Atomic-Scale Simulation Study. *J. Appl. Phys.* **1998**, *84*, 3895.

(20) Ramalingam, S.; Maroudas, D.; Aydil, E. S. Atomistic Simulation Study of the Interactions of SiH_3 Radicals with Silicon Surfaces. *J. Appl. Phys.* **1999**, *86*, 2872.

(21) Ramalingam, S.; Maroudas, D.; Aydil, E. S.; Walch, S. P. Abstraction of Hydrogen by SiH3 from Hydrogen-Terminated Si(001)−(2 × 1) Surfaces. *Surf. Sci.* **1998**, *418*, L8.

(22) Coltrin, M. E.; Moffatt, H. K.; Kee, R. J.; Rupley, F. M. CRESLAF, a Fortran Program for Modeling Laminar, Chemically Reacting, Boundary-Layer Flow in Cylindrical or Planar Channel, Sandia Lab., CHEMKIN Collection Release 3.6, 2001.

(23) Weerts, W. L. M.; de Croon, M. H. J. M.; Marin, G. B. The Adsorption of Silane, Disilane, and Trisilane on Polycrystalline Silicon: a Transient Kinetic Study. *Surf. Sci.* **1996**, *367*, 321.

(24) Bratu, P.; Kompa, K. L.; Hoffer, U. Optical Second-Harmonic Investigation of H_2 and D_2 Adsorption on Si(100) 2 × 1: Surface Temperature Dependence of the Sticking Coefficient. *Chem. Phys. Lett.* **1996**, *251*, 1.

(25) Bratu, P.; Hofer, U. Phonon-Assisted Sticking of Molecular Hydrogen on Si(111) 7 × 7. *Phys. Rev. Lett.* **1995**, *74*, 1625.

(26) Greve, D. W. Growth of Epitaxial Germanium−Silicon Heterostructures by Chemical Vapor Deposition. *Mater. Sci. Eng.* **1993**, *B18*, 22.

(27) Buss, R. J.; Ho, P.; Breiland, W. G.; Coltrin, M. E. Reactive Sticking Coefficients for Silane and Disilane on Polycrystalline Silicon. *J. Appl. Phys.* **1988**, *63*, 2808.

(28) Sinniah, K.; Sherman, M. G.; Lewis, L. B.; Weinberg, W. H.; Yates, J. T.; Janda, K. C. Hydrogen Desorption from the Monohydride Phase on Si(100). *J. Chem. Phys.* **1990**, *92*, 5700.

(29) Sinniah, K.; Sherman, M. G.; Lewis, L. B.; Weinberg, W. H.; Yates, J. T.; Janda, K. C. New Mechanism for Hydrogen Desorption from Covalent Surfaces: The Monohydride Phase on Si(100). *Phys. Rev. Lett.* **1989**, *62*, 567.

(30) Tsai, D. S.; Chang, T. C.; Hsin, W. C.; Hamamura, H.; Shimogaki, Y. Surface Reaction Probability of Radicals Correlated from Film Thickness Contours in Silane Chemical Vapor Deposition. Submitted for publication in *Thin Solid Films*.

Received for review August 30, 2001
Revised manuscript received February 8, 2002
Accepted February 17, 2002

IE0107183